Bioorganic & Medicinal Chemistry 20 (2012) 6552–6558

Contents lists available at SciVerse ScienceDirect

Bioorganic & Medicinal Chemistry

journal homepage: www.elsevier.com/locate/bmc

Synthesis and structure–activity relationship of berberine analogues in LDLR up-regulation and AMPK activation

Yan-Xiang Wang †, Wei-Jia Kong †, Ying-Hong Li, Sheng Tang, Zheng Li, Yang-Biao Li, Yong-Qiang Shan, Chong-Wen Bi, Jian-Dong Jiang *, Dan-Qing Song *

Institute of Medicinal Biotechnology, Chinese Academy of Medical Sciences and Peking Union Medical College, Beijing 100050, China

ARTICLE INFO

Article history:
Received 27 July 2012
Revised 17 September 2012
Accepted 17 September 2012
Available online 24 September 2012

Keywords:
Berberine
Metabolic syndrome
AMPK
LDLR
Structure–activity relationship

ABSTRACT

Currently there is no approved medicine for the treatment of metabolic syndrome. A series of new derivatives of berberine (BBR) or pseudoberberine (**1**) was synthesized and evaluated for their activity on AMP-activated protein kinase (AMPK) activation and up-regulatory low-density-lipoprotein receptor (LDLR) gene expression, respectively. In addition, the four major metabolites of BBR in vivo were also examined for their activity on AMPK in order to further understand the chemical mechanisms responsible for its glucose-lowering efficacy. Among those BBR analogues, compound **1** exhibited the potential effect on AMPK activation and LDLR up-regulation as compared with BBR. The results suggested that compound **1** might be a multiple-target agent for the treatment of metabolic syndrome, and thus was selected as a promising drug candidate for further development.

1. Introduction

Berberine (BBR, Fig. 1) is an isoquinoline natural product extracted from *Coptis chinensis*. It has been extensively used in China as a non-prescription drug for diarrhea for decades with a confirmed safety.[1,2] Our previous work has identified BBR as a new drug for hyperlipidemia causing reduction of cholesterol and triglycerides in hyperlipidemic patients with a novel mode of action different from the current statins.[3,4] The results were confirmed by other groups.[5–7] BBR increases low-density-lipoprotein receptor (LDLR) expression by stabilizing LDLR mRNA through activation of extracellular signal-regulated kinase (ERK) pathway.[3,4] In addition, clinical studies have shown a significant hypoglycemic effect of BBR in patients with type 2 diabetes.[8,9] Activation of AMP-activated protein kinase (AMPK) by BBR is considered one of the mechanisms responsible for its glucose-lowering.[10–14] Our findings suggest that BBR is a promising agent with great potential for the treatment of metabolic syndrome, which represents a group of metabolic disorders including insulin resistance, obesity, dyslipidemia, hypertension and low level of high-density-lipoprotein (HDL). However, currently there is no approved medicine for this complicated disease.[15]

In our previous study, the structure–activity relationship (SAR) analysis of BBR for the up-regulation of LDLR mRNA expression was basically elucidated.[16,17] Among the BBR derivatives, pseudoberberine (**1**, Fig 1) exhibited a potent lipid-lowing effect greater than BBR did in vitro as well as in vivo.[16,17] In searching for BBR analogues for the treatment of metabolic syndrome, the BBR compound library[16,17] was established in our laboratory and screened for AMPK activation, with BBR as a reference control. Through the screening, we found that compound **1** displayed a potential activity in activating AMPK.

In our continuing efforts of discovery new BBR derivatives for both LDLR up-regulation and AMPK activation, extensive structure–activity relationship (SAR) study was performed with BBR and **1** as the lead. SAR was carried out by focusing on the substituents on the aromatic ring A or D, and thus 14 BBR derivatives were designed, de novo synthesized and evaluated for their activities on AMPK activation and LDLR up-regulation. In order to further understand the chemical mechanisms of BBR responsible for its glucose-lowering efficacy, the four major metabolites of BBR were also examined for their activity on AMPK.

2. Chemistry

Fourteen BBR analogues were synthesized through a four-step process (Scheme 1), using commercially available derivatives of phenylethylamine (**2**) and benzaldehyde (**3**) as the starting materials with the methods reported previously.[16–18] In the intermolecular cyclization of the intermediate **5**, ring B and C of **6** could form

* Corresponding authors. Tel./fax: +86 10 6316 5268 (D.-Q.S.); tel.: +86 10 6318 8423; fax: +86 10 6301 7302 (J.-D.J.).
E-mail addresses: jiang.jdong@163.com (J.-D. Jiang), songdanqingsdq@hotmail.com (D.-Q. Song).
† These authors made equal contributions to the work.

0968-0896/$ - see front matter © 2012 Elsevier Ltd. All rights reserved.
http://dx.doi.org/10.1016/j.bmc.2012.09.029

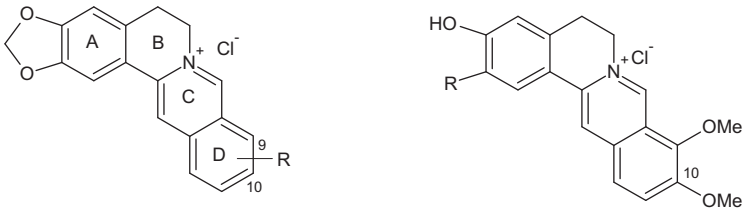

BBR: R = 9, 10-dimethoxy;
1: R = 10, 11-dimethoxy;
M1-a: R = 9-hydroxy, 10-methoxy;
M2: R = 9-methoxy, 10-hydroxy
M3: R = hydroxy;
M4: R = methoxy

Figure 1. Structures of BBR, compound **1**, M1-a, and M2–M4.

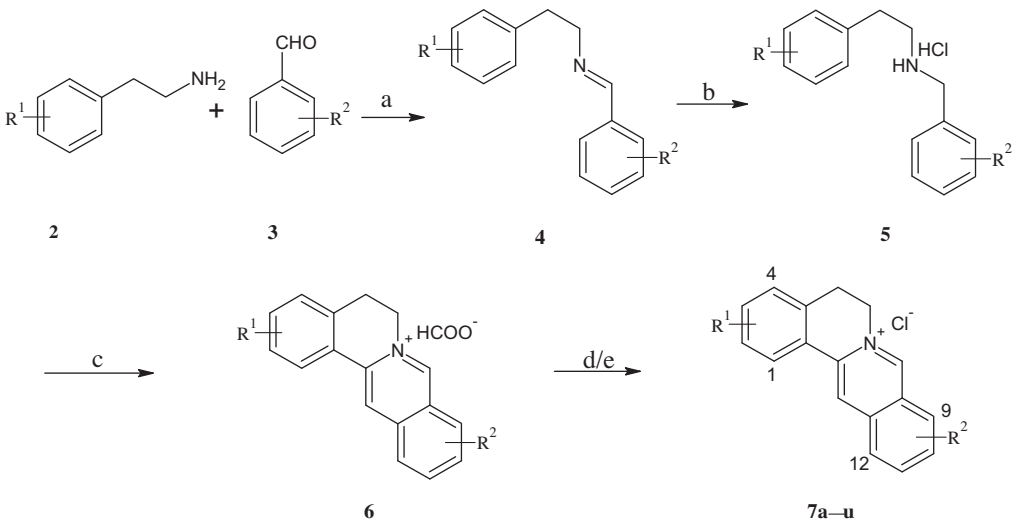

7a: R^1 = 2, 3-OCH_2O-; R^2= 10-OCH_3, 11-OC_2H_5;
7b: R^1 = 2, 3-OCH_2O-; R^2= 10, 11-OCH_2CH_2O-;
7c: R^1 = 2, 3-OCH_2O-; R^2= 9-Cl, 10-OCH_3, 11-OCH_3;
7d: R^1 = 2, 3-OCH_2O-; R^2= 9-Cl, 10-OCH_3;
7e: R^1 = 2, 3-OCH_2O-; R^2= 9-F, 10-OCH_3;
7f: R^1 = 2, 3-OCH_2O-; R^2= 9-OH, 10-OCH_3, 12-Br;
7g: R^1 = 2-OC_2H_5, 3-OCH_3; R^2= 9,10-dimethoxy;
7h: R^1 = 2-OCH_3, 3-OC_2H_5; R^2= 9,10-dimethoxy;
7i: R^1 = 1, 2, 3-tri-methoxy; R^2= 9,10-dimethoxy;
7j: R^1 = 3-OCH_3, 4-OCH_3; R^2= 9,10-dimethoxy;
7k: R^1 = 2-OH, 3-OCH_3; R^2= 9,10-dimethoxy;
7l: R^1 = 2-OC_2H_5, 3-OCH_3; R^2= 10,11-dimethoxy;
7m: R^1 =2-OCH_3, 3-OC_2H_5; R^2= 10,11-dimethoxy;
7n: R^1 = 3, 4-dimethoxy; R^2= 10,11-dimethoxy.

Scheme 1. Synthesis of the aimed compounds. Reagents and conditions: (a) 100 °C, 8 h; (b) $NaBH_4$, methanol, reflux, 5 h; (c) glyoxal, formic acid, $CuSO_4$, HCl, 100 °C, 6 h; (d) methanol/H_2O, CaO, rt, 2 h; (e) HCl.

according to Pictet–Spengler cyclization and Friedel–Crafts alkylation rule in one step, and subsequently the key intermediate **6** would be obtained with ideal yields (35–72%). The crude products in **7** series were prepared by the acidification of intermediate **6**. The final products (**7a**–**n**) were purified via flash column chromatography using methanol/dichloromethane as the gradient eluent.

3. Results and discussion

3.1. SAR analysis for the LDLR up-regulating activity

All the synthesized analogues were examined in human liver HepG2 cells for their activities on LDLR mRNA expression. The up-regulatory effect was quantitatively measured with real time RT-PCR assay. Structures of the analogues and their LDLR up-regulatory effects are shown in Table 1.

SAR analysis was first focused on the influence of substitutions on the ring D, by which six new BBR derivatives (**7a**–**f**) were prepared and tested. Replacement of OCH_3 with OC_2H_5 at the R^7 position of **1**, compound **7a** lost the activity on LDLR expression completely. Replacing by ethylenedioxy at the R^6 and R^7 positions of **1** (**7b**) did not generate ideal activity. Introducing chloride at position R^5 of **1** (**7c**) or replacing by chloride, fluorine or hydroxyl at the R^5 position of BBR (**7d**–**f**) almost lost their up-regulatory LDLR expression. It seems that di-methoxy at the R^5 and R^6 or at the R^6 and R^7 positions on the ring D might be essential for the activity on LDLR up-regulation.

Table 1
Structures and LDLR up-regulating activities of the synthesized compounds in HepG2 cells

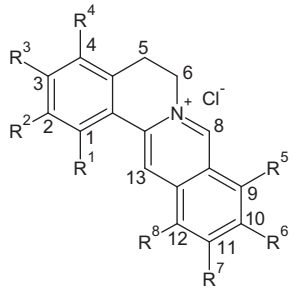

Compd	R^1	R^2	R^3	R^4	R^5	R^6	R^7	R^8	LDLR mRNA[a]
BBR	H	OCH_2O		H	OCH_3	OCH_3	H	H	2.35 ± 0.30
1	H	OCH_2O		H	H	OCH_3	OCH_3	H	3.23 ± 0.50*
7a	H	OCH_2O		H	H	OCH_3	OC_2H_5	H	0.91 ± 0.10
7b	H	OCH_2O		H	H	OCH_2	CH_2O	H	0.96 ± 0.10
7c	H	OCH_2O		H	Cl	OCH_3	OCH_3	H	0.92 ± 0.10
7d	H	OCH_2O		H	Cl	OCH_3	H	H	1.12 ± 0.10
7e	H	OCH_2O		H	F	OCH_3	H	H	1.00 ± 0.10
7f	H	OCH_2O		H	OH	OCH_3	H	Br	0.94 ± 0.10
7g	H	OC_2H_5	OCH_3	H	OCH_3	OCH_3	H	H	1.00 ± 0.10
7h	H	OCH_3	OC_2H_5	H	OCH_3	OCH_3	H	H	1.02 ± 0.10
7i	OCH_3	OCH_3	OCH_3	H	OCH_3	OCH_3	H	H	0.88 ± 0.10
7j	H	H	OCH_3	OCH_3	OCH_3	OCH_3	H	H	0.89 ± 0.10
7k	H	OH	OCH_3	H	OCH_3	OCH_3	H	H	1.15 ± 0.10
7l	H	OC_2H_5	OCH_3	H	H	OCH_3	OCH_3	H	0.96 ± 0.10
7m	H	OCH_3	OC_2H_5	H	H	OCH_3	OCH_3	H	1.04 ± 0.10
7n	H	H	OCH_3	OCH_3	H	OCH_3	OCH_3	H	0.92 ± 0.10

[a] Human liver HepG2 cells were treated with BBR analogues (10 μM) for 12 h. Abundances of LDLR mRNA were determined by real-time RT-PCR, with LDLR mRNA level in the untreated cells defined as 1. The data shown are the mean ± SEM of 3 separate experiments,*$p < 0.05$ vs BBR.

Next, the SAR study was conducted for the substituents on the ring A. Introducing methoxy, ethoxyl and/or hydroxyl at the R^1–R^4 positions in BBR (**7g**–**k**) abolished the activities partially or completely. Similarly, compounds **7l**–**n** bearing methoxy and/or ethoxyl at the R^2–R^4 positions in compound **1** showed no activities as well. The results were basically consistent with our previous SAR analysis.[16–18]

3.2. AMPK activation for the synthesized compounds

In parallel, AMPK activations of fourteen synthesized analogues (**7a**–**7n**) were examined in human liver HepG2 cells as well. Protein levels of phosphorylated AMPKα (*p*-AMPKα) and total AMPKα were determined by Western blot analysis (Fig. 2, upper panel). Compared to vehicle control (p <0.01), the ratio of *p*-AMPKα/AMPKα increased by 3.2 and 2.6-fold after BBR or compound **1** treatment, respectively (Fig. 2, lower panel), as proved by the increase of *p*-AMPKα level. However, all the study analogues lost their activities partially or completely in AMPK activation in comparison with BBR or compound **1**. We noticed that with an enhanced LDLR-upregulating activity, the stimulating effect of compound **1** on AMPK was close to that of BBR after normalization ($p > 0.05$). As BBR acts on LDLR through ERK pathway[3] and AMPK via mitochondria mechanism[12–14], we assume that BBR and its analogs, such as compound **1**, might have their own preference in selecting pathways due to difference in their structure.

To understand the chemical mechanisms of BBR responsible for glucose-lowering efficacy, four major metabolites of BBR, berberrubine (M1-a), thalifendine (M2), demethyleneberberine (M3) and jatrorrhizine (M4) (Fig. 1)[19,20] were also measured for their AMPK activation. M1-a may transform into its isomer (M1-b) in alkaline conditions (Fig. 3).[18a,21] Among the metabolites, M1-a or M1-b afforded the best effect in AMPK activation, although its activity was lower than that of parent BBR. Similarly, M1-a exhibited the best up-regulatory effect on LDLR mRNA expression among the four metabolites, lower than that of BBR.[22,23] The results suggest that BBR treats the risk factors of metabolic syndrome through its original compound in collaboration with its bioactive metabolites (Fig. 3, lower panel). As M1-a possesses a free arm at the 9-position (9-OH), it might be selected as an ideal parent of BBR to make prodrugs for improving the bioavailability and therapy efficacy in vivo.

3.3. AMPK activation of compound 1

Through SAR analysis, compound **1** possesses an optimal structure in AMPK activation, and thus was selected for further investigation of AMPK activating effect. Time and dose-correlative experiments were performed. HepG2 cells were treated with 10 μM of **1** for different time intervals (Fig. 4A) or treated with different concentrations of **1** for 4 h (Fig. 4B). Protein levels of *p*-AMPKα and total AMPKα were determined by Western blot. We found that compound **1** activates AMPK in a time- and dose-dependent manner, and the activity come up to the maximum value when HepG2 cells were treated about 4 h at the concentration of 10 μM. The activating effect of compound **1** on AMPK is also verified in another cell line, rat skeletal muscle L6 cells (data not shown). Therefore, compound **1** displayed a potent activity on both AMPK activation and LDLR expression, and thus was selected as a promising multiple-target candidate for metabolic syndrome treatment.

4. Conclusion

In conclusion, 14 BBR analogues defined on substituents of the ring A or D were synthesized and examined for their effects on

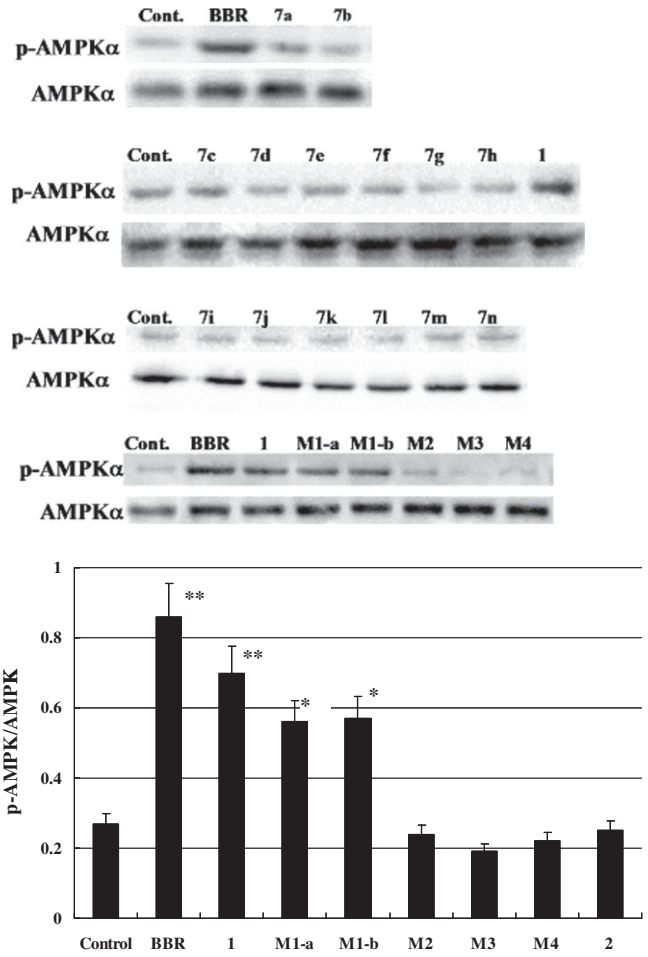

Figure 2. Activities of all BBR analogues on AMPK in cultured cells. HepG2 cells were treated with vehicle control or tested compounds at 10 μM for 4 h as indicated. Protein levels of *p*-AMPKα and total AMPKα were determined (upper panel). Bands were scanned and quantified; the percentages of *p*-AMPKα in total AMPKα were calculated and plotted (lower panel, some of the histograms were not shown). Values in the histogram were mean ± SEM of 3 repeated experiments. $^{*}p$ <0.05, $^{**}p$ <0.01 vs control.

LDLR up-regulation and AMPK activation with BBR or **1** as the leads, 'respectively'. The four major metabolites were evaluated for their AMPK activation as well. Out of those BBR analogues and metabolites, compound **1** activates AMPK in a time- and dose-dependent manner with an activity similar to that of BBR itself. In addition, it exhibited better LDLR up-regulating activity in vitro as well as in vivo than BBR did.[16] Therefore, compound **1** might become a promising multiple-target candidate for metabolic syndrome treatment, and has been selected for the next-step evaluation in animal experiments.

5. Experimental section

5.1. Chemistry

Unless otherwise noted, all commercial reagents and solvents were obtained from the commercial provider and used without further purification. ^{1}H NMR and ^{13}C NMR spectra were recorded on Varian 400 MHz spectrometer. Chemical shift was reported relative to internal tetramethylsilane (δ 0.00 ppm) or $(CD_3)_2SO$ (δ 2.50 ppm) for ^{1}H and $(CD_3)_2SO$ (δ 39.5 ppm) for ^{13}C. Flash column chromatography was performed on 200–400 mesh silica gel. Thin-layer chromatography (TLC) was performed using E. Merck silica gel 60 F254 precoated plates. IR was recorded on a Thermo FT/IR spectrophotometer Nicolet 5700. Melting point (mp) was uncorrected and recorded on a Büchi capillary melting point apparatus.

5.2. 5,6-Dihydro-9-oxo-10-methoxy-benzo[*g*]-1,3-benzodioxolo[5,6-*a*] quinolizinium (M1-b)

BBR (2.0 g, 5.38 mmol) was heated at 195–210 °C for 10–15 min under vacuum (20–30 mmHg) to afford dark wine solid which was re-crystallized with anhydrous ethanol twice, and then M1-b (1.26 g, 3.89 mmol, 72%) was obtained. Yellow solid; mp 195−196 °C; ^{1}H NMR δ: 9.10 (s, 1H), 8.00 (s, 1H), 7.60 (s, 1H), 7.23 (d, J = 8.0 Hz, 1H), 6.95 (s, 1H), 6.39 (d, J = 8.0 Hz, 1H), 6.08 (s, 2H), 4.48 (t, J = 6.0 Hz, 2H), 3.73 (s, 3H), 3.03 (t, J = 6.0 Hz, 2H); ^{13}C NMR δ: 149.5, 148.3, 147.3, 145.7, 133.3, 132.0, 129.3, 121.8, 121.4, 119.8, 117.2, 108.2, 104.7, 101.6 (2), 55.7 (2), 52.4, 27.4; IR (KBr) γ: 2904, 1634, 1569, 1509, 1475, 1392, 1287, 1219, 1033 cm^{-1}; HRMS-ESI: calcd for $C_{19}H_{15}NO_4$ $(M+H)^+$ 322.10793, found 322.10725.

5.3. Mutual transformation of M1-a and M1-b

M1-b (1.26 g, 3.89 mmol) was dissolved in ethanol, ethanol/concentrated HCl (95:5) were added portionwise to adjust pH to 5–6. The solution was concentrated in vacuo to afford the title compound M1-a[22] (1.15 g, 3.20 mmol, 82%) as yellow needles. ^{13}C NMR δ: 149.6, 147.6, 145.8, 145.3, 143.7, 136.6, 132.4, 125.5, 120.6, 119.8, 118.0, 117.6, 108.4, 105.3, 102.0, 57.0, 54.9, 26.4; IR (KBr) γ: 3347, 3049, 1508, 1354, 1330, 1281, 1262, 1101, 1035, 923 cm^{-1}.

M1-a (1.50 g, 4.17 mmol) was dissolved in methanol (50 mL). To this solution, K_2CO_3 (1.15 g, 8.35 mmol) was added; the mixture was stirred at the room temperature for 1 h and filtered. The filtrate was concentrated in vacuo to afford dark wine solid which was re-crystallized with anhydrous ethanol. M1-b (1.08 g, 3.33 mmol, 80%) was obtained.

5.4. General procedure to obtain final dibenzo-quinolizine analogues

The requisite substituted phenylethylamine and benzaldehyde were purchased commercially. A 250 mL round bottom flask was

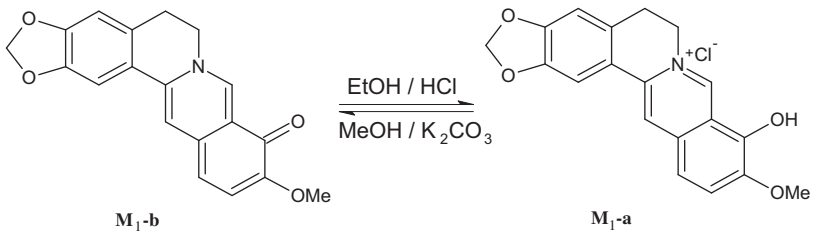

Figure 3. Mutual transformation of M1-a and M1-b.

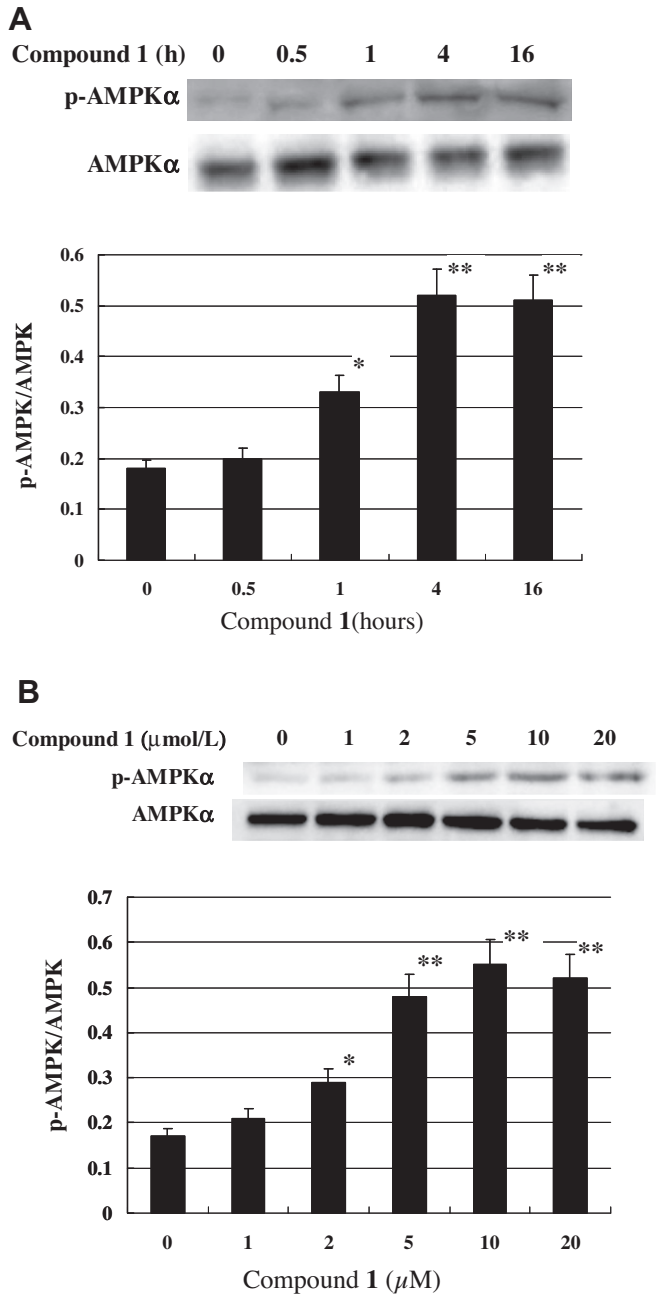

Figure 4. Time and dose-dependent activation of AMPK by compound **1**. HepG2 cells were treated with 10 μM of compound **1** for different time intervals (A) or treated with different concentrations of compound **1** for 4 h (B). Protein levels of *p*-AMPKα and total AMPKα were determined by western blot. Bands were scanned and quantified; the percentages of *p*-AMPKα in total AMPKα was calculated and plotted. Values in the histogram were mean ± SEM of 3 repeated experiments. $^{*}p$ <0.05, $^{**}p$ <0.01 vs untreated.

charged with the corresponding substituted phenylethylamine (**1**, 1.0 equiv) and substituted benzaldehyde (**2**, 1.0 equiv) at 70 °C, and the mixture was stirred under vacuum for 1 h. Then, 100 mL methanol was added to solve the residue. To this solution, $NaBH_4$ (3.0 equiv) was added portionwise at the room temperature. The mixture was stirred under gentle reflux for 4 h. Upon completion, as determined by TLC, the reaction mixture was concentrated in vacuo. The residue was dissolved in water (300 mL). The resulting aqueous phase was extracted with ethyl acetate (3 × 100 mL) and the combined organic layers were rinsed with saturated brines (100 mL), dried (Na_2SO_4). Concentrated hydrochloric acid was added dropwise to adjust pH of the organic layer to 5–6, and filter to give the hydrochlorate (**4**) without further purification.

To a suspension of anhydrous $CuSO_4$ (3.6 equiv) and corresponding hydrochlorate (**4**, 1.0 equiv) in anhydrous formic acid (45 mL) was added 40% glyoxal solution (2.0 equiv) at 100 °C. The reaction mixture was stirred at 100 °C for 5 h, concentrated hydrochloric acid (0.8 and 0.6 equiv) was added 'respectively' at 2 h and 4 h through this process. Upon completion, as determined by TLC, the mixture was filtered. The filtrate was concentrated in vacuo. The residue was dissolved in methanol (500 mL) and water (10 mL), CaO was added portionwise to adjust pH to 9–10. The suspension was stirred at the room temperature for 2 h, filtered and concentrated in vacuo. The resulting residue was purified via flash column chromatography using methanol/dichloromethane as the eluent to give **6**.

5.4.1. 5,6-Dihydro-10-methoxy-11-ethoxy-benzo[g]-1,3-benzodioxolo[5,6-a] quinolizinium (7a)

Yield: 78%; Light yellow solid; mp 261–263 °C; ^{1}H NMR δ: 9.54 (s, 1H), 8.74 (s, 1H), 7.71 (s, 2H), 7.56 (s, 1H), 7.09 (s, 1H), 6.16 (s, 2H), 4.76 (t, J = 6.0 Hz, 2H), 4.33 (q, J = 6.8 Hz, 2H), 3.99 (s, 3H), 3.18 (t, J = 6.0 Hz, 2H), 1.47 (t, J = 6.8 Hz, 3H); ^{13}C NMR δ: 156.7, 152.2, 149.8, 147.6, 145.5, 138.1, 136.6, 130.6, 122.0, 120.5, 118.2, 108.5, 106.6, 105.7, 105.3, 102.1, 65.2, 56.3, 54.4, 26.4, 14.2; IR (KBr) γ: 3413, 2981, 1616, 1502, 1444, 1373, 1217, 1034 cm^{-1}; HRMS-ESI: Calcd for $C_{21}H_{20}NO_4Cl$ $(M-Cl)^+$ 350.1392, found 350.1410.

5.4.2. 5,6-Dihydro-10,11-{2,3-dihydro[1,4]dioxino[2,3-g]}benzo[g]-1,3-benzodioxolo[5,6-a] quinolizinium (7b)

Yield: 77%; Yellow solid; mp 323–326 °C; ^{1}H NMR δ: 9.63 (s, 1H), 8.73 (s, 1H), 7.84 (s, 1H), 7.72 (s, 1H), 7.58 (s, 1H), 7.08 (s, 1H), 6.16 (s, 2H), 4.75 (t, J = 6.0 Hz, 2H), 4.56 (t, J = 3.2 Hz, 2H), 4.49 (t, J = 3.2 Hz, 2H), 3.17 (t, J = 6.0 Hz, 2H); ^{13}C NMR δ: 152.9, 149.7, 147.6, 147.1, 147.2, 137.5, 135.3, 130.5, 121.7, 120.5, 118.2, 114.0, 108.4, 105.3, 105.3, 102.0, 65.1, 64.2, 54.7, 26.4; IR (KBr) γ: 3257, 2992, 1635, 1503, 1440, 1375, 1289, 1190, 1034, 910 cm^{-1}; HRMS-ESI: Calcd for $C_{20}H_{16}NO_4Cl$ $(M-Cl)^+$ 334.1079, found 334.1075.

5.4.3. 5,6-Dihydro-9-chloro-10,11-dimethoxy-benzo[g]-1,3-benzodioxolo[5,6-a] quinolizinium (7c)

Yield: 75%; Bright yellow solid; mp 218–221 °C (decomp); ^{1}H NMR δ: 9.79 (s, 1H), 8.94 (s, 1H), 7.77 (s, 1H), 7.71 (s, 1H), 7.11 (s, 1H), 6.19 (s, 2H), 4.94 (t, J = 6.4 Hz, 2H), 4.14 (s, 3H), 3.98 (s, 3H), 3.21 (t, J = 6.4 Hz, 2H); ^{13}C NMR δ: 160.4, 149.6, 147.7, 145.0, 139.9, 138.3, 131.4, 124.2, 120.0, 119.6, 118.8, 108.5, 105.9, 105.5, 102.2, 61.2, 57.3, 54.5, 26.2, 18.5; IR (KBr) γ: 3272, 2992, 2946, 1636, 1504, 1483, 1419, 1374, 1267, 1222, 1035, 1007 cm^{-1}; HRMS-ESI: Calcd for $C_{20}H_{17}NO_4Cl_2$ $(M-Cl)^+$ 370.0846, found 370.0855.

5.4.4. 5,6-Dihydro-9-chloro-10-methoxy-benzo[g]-1,3-benzodioxolo[5,6-a] quinolizinium (7d)

Yield: 82%; Yellow solid; mp 185–187 °C (decomp); ^{1}H NMR δ: 9.94 (s, 1H), 9.05 (s, 1H), 8.25 (s, 2H), 7.81 (s, 1H), 7.10 (s, 1H), 6.18 (s, 2H), 4.99 (t, J = 6.4 Hz, 2H), 4.13 (s, 3H), 3.22 (t, J = 6.4 Hz, 2H); ^{13}C NMR δ: 155.3, 150.1, 147.7, 145.9, 138.4, 134.3, 131.0, 128.2, 125.0, 124.5, 120.9, 120.1, 115.8, 108.4, 105.5, 102.2, 57.5, 55.4, 26.1; IR (KBr) γ: 3362, 3022, 1621, 1504, 1366, 1343, 1277, 1219, 1038 cm^{-1}; HRMS-ESI: calcd for $C_{19}H_{15}NO_3Cl_2$ $(M-Cl)^+$ 340.0740, found 340.0767.

5.4.5. 5,6-Dihydro-9-fluoro-10-methoxy-benzo[g]-1,3-benzodioxolo[5,6-*a*] quinolizinium (7e)

Yield: 73%; Orange solid; mp 251–253 °C (decomp); ^{1}H NMR δ: 10.08 (s, 1H), 9.03 (s, 1H), 8.29 (t, J = 8.8 Hz, 1H), 8.09 (d, J = 8.8 Hz, 1H), 7.80 (s, 1H), 7.09 (s, 1H), 6.18 (s, 2H), 4.93 (t, J = 6.4 Hz, 2H), 4.10 (s, 3H), 3.21 (t, J = 6.4 Hz, 2H); ^{13}C NMR δ: 150.8, 148.5, 146.3, 144.7, 138.9, 133.1, 131.6, 127.9, 125.3, 121.0, 120.9, 117.7, 109.2, 106.2, 102.9, 58.2, 56.1, 49.3, 26.9; IR (KBr) γ: 3187, 3004, 1623, 1611, 1504, 1393, 1367, 1283, 1225, 1103, 1035 cm^{-1}; HRMS-ESI: Calcd for $C_{19}H_{15}NO_3FCl$ $(M-Cl)^+$ 324.1036, found 324.1019.

5.4.6. 5,6-Dihydro-10-methoxy-12-bromo-benzo[*g*]-1,3-benzodioxolo[5,6-*a*] quinolizinium-9-ol (7f)

Yield: 51%; Brown solid; mp 135−137 °C (decomp); ^{1}H NMR δ: 10.00 (s, 1H), 8.41 (s, 1H), 8.38 (s, 1H), 7.89 (s, 1H), 7.07 (s, 1H), 6.17 (s, 2H), 4.89 (t, J = 6.0 Hz, 2H), 4.06 (s, 3H), 3.17 (t, J = 6.0 Hz, 2H); ^{13}C NMR δ: 156.3, 153.0, 151.0, 138.7, 136.4, 133.1, 130.3, 129.2, 127.3, 126.9, 123.3, 122.1, 117.0, 107.6, 104.5, 59.6, 55.3, 36.1, 25.6; IR (KBr) γ: 3150, 2922, 1596, 1503, 1493, 1315, 1277, 1261, 1097, 1031 cm^{-1}; HRMS-ESI: calcd for $C_{19}H_{15}NO_4BrCl$ $(M-Cl)^+$ 400.0184, found 400.0148.

5.4.7. 3,9,10-Trimethoxy-2-ethoxy-5,6-dihydroisoquinolino[2,1-*b*]isoquinolin-7-ium (7g)

Yield: 69%; Orange solid; mp 224–226 °C; ^{1}H NMR δ: 9.89 (s, 1H), 9.08 (s, 1H), 8.20 (d, J = 9.2 Hz, 1H), 8.03 (d, J = 9.2 Hz, 1H), 7.71 (s, 1H), 7.06 (s, 1H), 4.95 (t, J = 6.0 Hz, 2H), 4.12 (q, J = 6.8 Hz, 2H), 4.09 (s, 3H), 4.06 (s, 3H), 3.93 (s, 3H), 3.21 (t, J = 6.0 Hz, 2H), 1.37 (t, J = 6.8 Hz, 3H); ^{13}C NMR δ: 150.7, 150.2, 148.8, 145.4, 143.6, 137.7, 133.1, 128.6, 126.8, 123.4, 121.3, 119.8, 118.8, 112.0, 108.8, 64.0, 61.9, 57.0, 56.0, 55.3, 25.9, 14.6; IR (KBr) γ: 3338, 2978, 1605, 1525, 1511, 1456, 1364, 1274, 1244, 1215, 1109 cm^{-1}; HRMS-ESI: alcd for $C_{22}H_{24}NO_4Cl$ $(M-Cl)^+$ 366.1705, found 366.1675.

5.4.8. 2,9,10-Trimethoxy-3-ethoxy-5,6-dihydroisoquinolino[2,1-*b*]isoquinolin-7-ium (7h)

Yield: 76%; Orange solid; mp 208−211 °C (decomp); ^{1}H NMR δ: 9.88 (s, 1H), 9.03 (s, 1H), 8.20 (d, J = 9.2 Hz, 1H), 8.02 (d, J = 9.2 Hz, 1H), 7.70 (s, 1H), 7.08 (s, 1H), 4.93 (t, J = 5.6 Hz, 2H), 4.20 (q, J = 6.8 Hz, 2H), 4.09 (s, 3H), 4.07 (s, 3H), 3.86 (s, 3H), 3.23 (t, J = 5.6 Hz, 2H), 1.40 (t, J = 6.8 Hz, 3H); ^{13}C NMR δ: 151.6, 150.2, 147.9, 145.4, 143.6, 137.7, 133.1, 128.6, 126.7, 123.4, 121.3, 119.8, 118.9, 111.3, 109.8, 64.4, 61.9, 57.0, 55.8, 55.3, 25.9, 14.6; IR (KBr) γ: 3358, 2975, 2942, 1605, 1511, 1455, 1363, 1274, 1242, 1108 cm^{-1}; HRMS-ESI: Calcd for $C_{22}H_{24}NO_4Cl$ $(M-Cl)^+$ 366.1705, found 366.1676.

5.4.9. 1,2,3,9,10-Pentamethoxy-5,6-dihydroisoquinolino[2,1-*b*]isoquinolin-7-ium (7i)

Yield: 39%; Brown solid; mp 191−194 °C (decomp); ^{1}H NMR δ: 9.93 (s, 1H), 9.00 (s, 1H), 8.18 (s, 2H), 6.99 (s, 1H), 4.90 (t, J = 6.4 Hz, 2H), 4.09 (s, 3H), 4.07 (s, 3H), 3.90 (s, 3H), 3.87 (s, 3H), 3.83 (s, 3H), 3.19 (t, J = 6.4 Hz, 2H); ^{13}C NMR δ: 155.4, 152.1, 150.5, 145.4, 143.5, 141.2, 135.0, 133.2, 132.7, 126.5, 124.1, 123.0, 121.1, 113.0, 107.7, 61.9, 61.2, 60.7, 57.1, 56.2, 55.4, 27.3; IR (KBr) γ: 3374, 2941, 2839, 1596, 1504, 1461, 1358, 1273, 1113, 1041 cm^{-1}; HRMS-ESI: Calcd for $C_{22}H_{24}NO_5Cl$ $(M-Cl)^+$ 382.1654, found 382.1658.

5.4.10. 3,4,9,10-Tetramethoxy-5,6-dihydroisoquinolino[2,1-*b*]isoquinolin-7-ium (7j)

Yield: 72%; Bright yellow solid; mp 216–218 °C (decomp); ^{1}H NMR δ: 9.94 (s, 1H), 9.01 (s, 1H), 8.21 (d, J = 9.2 Hz, 1H), 8.07 (d, J = 9.2 Hz, 1H), 8.00 (d, J = 8.8 Hz, 1H), 7.28 (d, J = 8.8 Hz, 1H), 4.96 (t, J = 6.4 Hz, 2H), 4.10 (s, 3H), 4.08 (s, 3H), 3.94 (s, 3H), 3.81 (s, 3H), 3.27 (t, J = 6.4 Hz, 2H); ^{13}C NMR δ: 154.6, 150.3, 145.3, 144.9, 143.6, 137.6, 133.0, 128.9, 126.7, 123.6, 122.5, 121.5, 120.6, 120.1, 112.4, 61.9, 60.3, 57.0, 56.1, 54.8, 20.6; IR (KBr) γ: 3358, 2944, 1601, 1508, 1455, 1358, 1338, 1284, 1228, 1125, 1036 cm^{-1}; HRMS-ESI: Calcd for $C_{21}H_{22}NO_4Cl$ $(M-Cl)^+$ 352.1549, found 352.1525.

5.4.11. 2-Hydroxyl-3,9,10-trimethoxy-5,6-dihydroisoquinolino[2,1-*b*]isoquinolin-7-ium (7k)

Yield: 43%; Brown solid; mp 219−221 °C (decomp); ^{1}H NMR δ: 9.35 (s, 1H), 8.57 (s, 1H), 7.97 (s, 1H), 7.56 (s, 1H), 7.50 (s, 1H), 7.44 (s, 1H), 6.54 (s, 1H), 4.66 (t, J = 6.0 Hz, 2H), 4.03 (s, 3H), 3.96 (s, 3H), 3.85 (s, 3H), 3.04 (t, J = 6.0 Hz, 2H); ^{13}C NMR δ: 150.6, 150.2, 146.4, 145.4, 143.5, 137.8, 133.1, 127.0, 126.7, 123.6, 121.3, 119.5, 119.1, 112.2, 111.4, 61.9, 57.0, 55.9, 55.5, 25.9; IR (KBr) γ: 2939, 2840, 1604, 1363, 1274, 1246, 1105, 1026 cm^{-1}; HRMS-ESI: Calcd for $C_{20}H_{20}NO_4Cl$ $(M-Cl)^+$ 338.1392, found 338.1361.

5.4.12. 3,10,11-Trimethoxy-2-ethoxy-5,6-dihydroisoquinolino[2,1-*b*]isoquinolin-7-ium (7l)

Yield: 71%; Yellow solid; mp 220–222 °C; ^{1}H NMR δ: 9.56 (s, 1H), 8.86 (s, 1H), 7.71 (s, 1H), 7.66 (s, 1H), 7.60 (s, 1H), 7.07 (s, 1H), 4.78 (t, J = 6.4 Hz, 2H), 4.12 (q, J = 6.8 Hz, 2H), 4.07 (s, 3H), 3.99 (s, 3H), 3.93 (s, 3H), 3.20 (t, J = 6.4 Hz, 2H), 1.37 (t, J = 6.8 Hz, 3H); ^{13}C NMR δ: 157.4, 152.1, 150.7, 148.7, 145.5, 138.3, 136.6, 128.5, 122.0, 118.8, 117.9, 112.0, 108.5, 106.5, 105.3, 64.0, 56.6, 56.3, 56.0, 54.6, 26.4, 14.6; IR (KBr) γ: 3423, 2977, 1607, 1515, 1498, 1431, 1360, 1278, 1262, 1218, 1132 cm^{-1}; HRMS-ESI: Calcd for $C_{22}H_{24}NO_4Cl$ $(M-Cl)^+$ 366.1705, found 366.1672.

5.4.13. 2,10,11-Trimethoxy-3-ethoxy-5,6-dihydroisoquinolino[2,1-*b*]isoquinolin-7-ium (7m)

Yield: 86%; Yellow solid; mp 238−241 °C; ^{1}H NMR δ: 9.55 (s, 1H), 8.84 (s, 1H), 7.70 (s, 1H), 7.65 (s, 1H), 7.60 (s, 1H), 7.09 (s, 1H), 4.78 (t, J = 6.0 Hz, 2H), 4.19 (q, J = 6.8 Hz, 2H), 4.07 (s, 3H), 3.99 (s, 3H), 3.87 (s, 3H), 3.21 (t, J = 6.0 Hz, 2H), 1.40 (t, J = 6.8 Hz, 3H); ^{13}C NMR δ: 157.4, 152.2, 151.6, 147.8, 145.5, 138.4, 136.6, 128.5, 122.0, 118.9, 117.9, 111.4, 109.5, 106.5, 105.3, 64.2, 56.6, 56.3, 55.8, 54.6, 26.1, 14.7; IR (KBr) γ: 3389, 2975, 1607, 1515, 1497, 1465, 1430, 1360, 1277, 1216, 1128 cm^{-1}; HRMS-ESI: Calcd for $C_{22}H_{24}NO_4Cl$ $(M-Cl)^+$ 366.1705, found 366.1678.

5.4.14. 3,4,10,11-Tetramethoxy-5,6-dihydroisoquinolino[2,1-*b*]isoquinolin-7-ium (7n)

Yield: 78%; Bright green solid; mp 241−243 °C; ^{1}H NMR δ: 9.60 (s, 1H), 8.80 (s, 1H), 7.93 (d, J = 8.8 Hz, 1H), 7.27 (d, J = 8.8 Hz, 1H), 7.71 (s, 1H), 7.66 (s, 1H), 4.78 (t, J = 6.4 Hz, 2H), 4.06 (s, 3H), 3.99 (s, 3H), 3.93 (s, 3H), 3.79 (s, 3H), 3.25 (t, J = 6.4 Hz, 2H); ^{13}C NMR δ: 157.4, 154.6, 152.2, 145.4, 145.0, 138.3, 136.6, 128.9, 122.3, 122.2, 120.1, 118.1, 112.4, 106.5, 105.4, 60.3, 56.7, 56.3, 56.1, 54.2, 20.7; IR (KBr) γ: 3386, 3016, 2946, 1600, 1501, 1477, 1460, 1432, 1348, 1292, 1279, 1216, 1149, 1065, 1001 cm^{-1}; HRMS-ESI: Calcd for $C_{21}H_{22}NO_4Cl$ $(M-Cl)^+$ 352.1549, found 352.1521.

5.5. Biology

5.5.1. Cell culture

HepG2 cells were maintained in minimum essential medium (Gibco-Invitrogen, Grand Island, NY) containing 10% fetal bovine serum (FBS) and antibiotics. Cells were cultured in an atmosphere of 5% CO_2 at 37 °C. One day before experiment, cells were trypsinized and allowed to grow to about 70% confluence.

5.5.2. Western blot

After treatment, cells were harvested; total protein content of the cells was extracted as previously reported.[14] The whole cell

lysates were subjected to sodium dodecyl sulfate polyacrylamide gel electrophoresis and transferred onto the Hybond ECL Nitrocellulose Membranes (GE Healthcare, UK) through a Semi-Dry Transfer Cell (Bio-Rad, Hercules, CA). After blocking, a rabbit monoclonal antibody against the Thr172-phosphorylated AMPKα (Cell Signaling Technology, Inc., Danvers, MA) was used to detect the p-AMPKα level. After incubation with a horseradish peroxidase-conjugated goat anti-rabbit IgG (Cell Signaling Technology, Inc.), band signals were visualized with the Immobilon Western Chemiluminescent HRP Substrate (Millipore, Billerica, MA). The membranes were stripped; total AMPKα was examined by a rabbit monoclonal antibody (Cell Signaling Technology, Inc.). Bands were scanned and quantified using the Kodak 1D Image Analysis Software (Eastman Kodak Company, Rochester, NY). *p*-AMPKα protein levels were normalized to that of total AMPKα and plotted as indicated.

5.5.3. RNA isolation and real-time RT-PCR

Total RNAs were isolated from cells using the TRIzol Reagent (Invitrogen, Carlsbad, CA) according to the supplier's protocol. For reverse transcription, 0.2 μg of total RNA was used as a template in a 20 μL reaction system containing random primers and the AMV reverse transcriptase (Promega, Madison, WI). The reverse transcription reactions were conducted at 42 °C for 15 min and then inactivated at 95 °C for 5 min. Quantitative real-time PCR was performed using the iQ5 Multicolor Real-Time PCR Detection System (Bio-Rad, Hercules, CA) as described before[15]. Each experiment was repeated at least 3 times. β-Actin was used as internal control for relative quantification of target gene using the comparative threshold cycle method. Normalized mRNA expression levels were plotted as fold of untreated control, which was designated as 1.

5.5.4. Statistical analysis

After validation of the test for homogeneity of variance, differences among study groups were determined by one-way ANOVA followed by the Newman–Keuls test for multiple comparisons.

Acknowledgment

This work was supported by the National Natural Science Foundation of China (90913002) and the National S&T Major Special Project on Major New Drug Innovation (2012ZX09301002−001). We also thank Dr. Partrick Bartlow for his critical review of the manuscript.

References and notes

1. Luo, L. J. *Chin. J. Med.* **1955**, *41*, 452.
2. Lau, C. W.; Yao, X. Q.; Chen, Z. Y.; Ko, W. H.; Huang, Y. *Cardiovasc. Drug Rev.* **2001**, *19*, 234.
3. Kong, W. J.; Abidi, P.; Lin, M.; Inaba, S.; Li, C.; Wang, Y.; Wang, Z.; Si, S.; Pan, H.; Wang, S.; Wu, J.; Wang, Y.; Li, Z.; Liu, J.; Jiang, J. D. *Nat. Med.* **2004**, *10*, 1344.
4. Kong, W. J.; Liu, J.; Jiang, J. D. *J. Mol. Med. (Berl)* **2006**, *84*, 29.
5. Zhang, Y.; Li, X.; Zou, D.; Liu, W.; Yang, J.; Zhu, N.; Huo, L.; Wang, M.; Hong, J.; Wu, P.; Ren, G.; Ning, G. *J. Clin. Endocrinol. Metab.* **2008**, *93*, 2559.
6. Cicero, A. F.; Rovati, L. C.; Setnikar, I. *Arzneimittelforschung* **2007**, *57*, 26.
7. Yin, J.; Xing, H.; Ye, J. *Metabolism* **2008**, *57*, 712.
8. González-Sánchez, J. L.; Serrano-Ríos, M. *Drug News Perspect.* **2007**, *20*, 527.
9. Stumvoll, M.; Goldstein, B. J.; Van Haeften, T. W. *Lancet* **2005**, *365*, 1333.
10. Zhang, H.; Wei, J.; Xue, R.; Wu, J. D.; Zhao, W.; Wang, Z. Z.; Wang, S. K.; Zhou, Z. X.; Song, D. Q.; Wang, Y. M.; Pan, H. N.; Kong, W. J.; Jiang, J. D. *Metabolism* **2010**, *59*, 285.
11. Kong, W. J.; Zhang, H.; Song, D. Q.; Xue, R.; Zhao, W.; Wei, J.; Wang, Y. M.; Shan, N.; Zhou, Z. X.; Yang, P.; You, X. F.; Li, Z. R.; Si, S. Y.; Zhao, L. X.; Pan, H. N.; Jiang, J. D. *Metabolism* **2009**, *58*, 109.
12. Kim, W. S.; Lee, Y. S.; Cha, S. H.; Jeong, H. W.; Choe, S. S.; Lee, M. R.; Oh, G. T.; Park, H. S.; Lee, K. U.; Lane, M. D.; Kim, J. B. *Am. J. Physiol. Endocrinol. Metab.* **2009**, *296*, 812.
13. Lee, Y. S.; Kim, W. S.; Kim, K. H.; Yoon, M. J.; Cho, H. J.; Shen, Y.; Ye, J. M.; Lee, C. H.; Oh, W. K.; Kim, C. T.; Hohnen-Behrens, C.; Gosby, A.; Kraegen, E. W.; James, D. E.; Kim, J. B. *Diabetes* **2006**, *55*, 2256.
14. Yin, J.; Gao, Z.; Liu, D.; Liu, Z.; Ye, J. *Am. J. Physiol. Endocrinol. Metab.* **2008**, *294*, 148.
15. Zimmet, P.; Alberti, K. G.; Shaw, J. *Nature* **2001**, *414*, 782.
16. Yang, P.; Song, D. Q.; Li, Y. H.; Kong, W. J.; Wang, Y. X.; Gao, L. M.; Liu, S. Y.; Cao, R. Q.; Jiang, J. D. *Bioorg. Med. Chem. Lett.* **2008**, *18*, 4675.
17. (a) Wang, Y. X.; Wang, Y. P.; Zhang, H.; Kong, W. J.; Li, Y. H.; Liu, F.; Gao, R. M.; Liu, T.; Jiang, J. D.; Song, D. Q. *Bioorg. Med. Chem. Lett.* **2009**, *19*, 6004; (b) Li, Y. H.; Yang, P.; Kong, W. J.; Wang, Y. X.; Hu, C. Q.; Zuo, Z. Y.; Wang, Y. M.; Gao, H.; Gao, L. M.; Feng, Y. C.; Du, N. N.; Liu, Y.; Song, D. Q.; Jiang, J. D. *J. Med. Chem.* **2009**, *52*, 492.
18. (a) Maurice, S.; Mohammad, R. *J. Nat. Prod.* **1986**, *49*, 398; (b) Wang, L. J.; Ye, X. L.; Li, X. G.; Sun, Q. L.; Yu, G.; Cao, X. G.; Liang, Y. T.; Zhang, H. S.; Zhou, J. Z. *Planta Med.* **2008**, *74*, 290; (c) Wright, C. W.; Marshall, S. J.; Russell, P. F.; Anderson, M. M.; Phillipson, J. D.; Kirby, G. C.; Warhurst, D. C.; Schiff, P. L. *J. Nat. Prod.* **2000**, *63*, 1638; (d) Sanders, M. M.; Liu, A. A.; Li, T. K.; Wu, H. Y.; Desai, S. D.; Mao, Y.; Rubin, E. H.; LaVoie, E. J.; Makhey, D.; Liu, L. F. *Biochem. Pharmacol.* **1998**, *56*, 1157.
19. Zuo, F.; Nakamura, N.; Akao, T.; Hattori, M. *Drug Metab. Dispos.* **2006**, *34*, 2064.
20. Qiu, F.; Zhu, Z.; Kang, N.; Piao, S.; Qin, G.; Yao, X. *Drug Metab. Dispos.* **2008**, *36*, 2159.
21. Park, K. D.; Cho, S. J.; Moon, J. S.; Kim, S. U. *Bioorg. Med. Chem. Lett.* **2010**, *20*, 6551.
22. Li, Y. H.; Li, Y.; Yang, P.; Kong, W. J.; You, X. F.; Ren, G.; Deng, H. B.; Wang, Y. M.; Wang, Y. X.; Song, D. Q.; Jiang, J. D. *Bioorg. Med. Chem.* **2010**, *18*, 6422.
23. Li, Y.; Ren, G.; Wang, Y. X.; Kong, W. J.; Yang, P.; Wang, Y. M.; Li, Y. H.; Yi, H.; Li, Z. R.; Song, D. Q.; Jiang, J. D. *J. Transl. Med.* **2011**, *9*, 62.